J. Membrane Biol. 60, 1–20 (1981)

The Journal of
Membrane Biology

Models of Coupled Salt and Water Transport Across Leaky Epithelia

Alan M. Weinstein and John L. Stephenson

Section on Theoretical Biophysics, National Heart, Lung and Blood Institute, and Mathematical Research Branch, National Institute of Arthritis, Metabolism, and Digestive Diseases, National Institutes of Health, Bethesda, Maryland 20205

Summary. A general formulation is presented for the verification of isotonic transport and for the assignment of a degree of osmotic coupling in any epithelial model. In particular, it is shown that the concentration of the transported fluid in the presence of exactly equal bathing media is, in general, not a sufficient calculation by which to decide the issue of isotonicity of transport. Within this framework, two epithelial models are considered: (1) A nonelectrolyte compartment model of the lateral intercellular space is presented along with its linearization about the condition of zero flux. This latter approximate model is shown to be useful in the estimation of deviation from isotonicity, intraepithelial solute polarization effects, and the capacity to transport water against a gradient. In the case of uphill water transport, some limitations of a model of fixed geometry are indicated and the advantage of modeling a compliant interspace is suggested. (2) A comprehensive model of cell and channel is described which includes the major electrolytes and the possible presence of intraepithelial gradients. The general approach to verification of isotonicity is illustrated for this numerical model. In addition, the insights about parameter dependence gained from the linear compartment model are shown to be applicable to understanding this large simulation.

Key words: isotonic epithelial transport, lateral intercellular space, linearized Kedem-Katchalsky equations, intraepithelial solute polarization

Glossary

Subscripts

Compartments

M Mucosal bath
S Serosal bath
E Extracellular channel

Membranes

A Tight junction
L Lateral membrane bounding the intercellular space
M Composite mucosal membrane comprised of tight junction and lateral membrane
B Basement membrane

Intensive Variables

($\alpha = M$, S or E references compartment subscripts)

C_0 Reference salt concentration, mOsm/cm^3
C_α Difference from reference, C_0, of salt concentration in compartment α, mOsm/cm^3
P_α Hydrostatic pressure, mmHg
$\bar{C}_i$ Mucosal impermeant species concentration, mOsm/cm^3

Membrane Properties

(β refers to any membrane subscript)

A_β Membrane area, cm^2
$L_{p\beta}$ Hydraulic conductivity, cm/sec mmHg
L_β ($= A_\beta \cdot L_{p\beta}$) Hydraulic conductivity, cm^3/sec mmHg
σ_β Reflection coefficient
h_β Salt permeability, cm/sec
H_β ($= A_\beta \cdot h_\beta$) Salt permeability, cm^3/sec
$\bar{C}_\beta$ Difference of mean membrane salt concentration from the reference C_0, mOsm/cm^3
L_p Epithelial hydraulic conductivity, cm^3/sec mmHg
σ Epithelial reflection coefficient
H Epithelial salt permeabilty, cm^3/sec

$$L_{LB} = \frac{L_L L_B}{L_L + L_B} \qquad L_{MB} = \frac{L_M L_B}{L_M + L_B}$$

Flows

(β refers to any membrane subscript)

$J_{v\beta}$ Transmembrane volume flow, cm^3/sec
$J_{s\beta}$ Transmembrane salt flux, mOsm/sec

0022-2631/81/0060-0001 $04.00

N Metabolically driven salt transport into the lateral intercellular space, mOsm/sec
J_v Transepithelial volume flow, cm^3/sec
J_s Transepithelial salt flux, mOsm/sec

Derived Variables

C_R Ratio of transepithelial salt flux to water flow (reabsorbate concentration), mOsm/cm^3
γ Osmotic coupling coefficient, (C_0/C_R)
C_M^* Mucosal equilibrium concentration - mucosal deviation from reference for which reabsorbate concentration is equal to mucosal bath concentration (serosa at reference), mOsm/cm^3
C_S^* Serosal equilibrium concentration - serosal deviation from reference for which reabsorbate concentration is equal to serosal bath concentration (mucosa at reference), mOsm/cm^3
C^* Mucosal deviation from reference for which reabsorbate concentration is equal to the reference concentration (serosa at reference), mOsm/cm^3
$\hat{C}$ Strength of transport - maximum salt gradient against which volume can be transported, mOsm/cm^3

The mechanism of coupling of solvent and solute fluxes in epithelial transport has been a central problem in epithelial physiology. Investigations into this issue typically involve a transporting epithelium suspended between mucosal and serosal bathing media and serial observations of the volume and composition of each bath. For the so-called "leaky" epithelia, two observations are held with certainty: (1) the epithelium is capable of transporting water up a chemical potential step (Diamond, 1964*a*; Whitlock & Wheeler, 1964) and (2) between equiosmolar bathing media the epithelium will transport solution so as to maintain identical tonicities of each bath within the limits of experimental observation (approximately 2%) (Diamond, 1964*b*; Whitlock & Wheeler, 1964). This has been termed "isotonic transport" and is found even as the osmolality of both bathing media is simultaneously varied over a wide range.

Neither of these observations is strictly compatible with modeling an epithelium as a single membrane described by the phenomenological equations of Kedem and Katchalsky. Such a model can transport NaCl against a chemical gradient but is incapable of uphill water transport. With a sufficiently large water permeability, volume flow could be accounted for by an osmotic force too small to be detected experimentally, but (with certain exceptions discussed below) measured water permeabilities have been too small to allow such a simple interpretation.

Consequently several mathematical models of varying complexity and comprehensiveness that allow active transport of NaCl across the baso-lateral cell surface to power transepithelial water transport have been proposed. Even in the simplest models, however, essential nonlinearities (in the state variables) of solute-solvent coupling have severely limited analytic reduction. The understanding of such models has often been dependent upon observations on numerical experiments, i.e. parameter variation. In this paper, after reviewing this hierarchy of models, we develop a general mathematical framework for their comparison. Within this framework we reconsider in detail a simple compartmental model and show that a linear analysis of such a model yields an accurate approximation when bathing media are nearly equal. Then, within the general framework, we examine a polyelectrolyte, distributed parameter, epithelial model. It is shown that the linearized compartment model yields important qualitative insight into the behavior of the comprehensive epithelial simulation.

In contrast to previous expositions of isotonically transporting epithelia, our approach emphasizes the behavior of epithelial models when the composition of the bathing media is varied. The effects of solute-solvent coupling are manifest in simulations of water transport between equal media or against an osmotic gradient as well as in simulations of attempts to drive transepithelial water flow by the imposition of osmotic gradients (L_p determinations). The assessment of model adequacy must be made in view of model predictions for all of these experimental maneuvers.

Background of the Problem

Curran and MacIntosh (1962) demonstrated that solute input into a compartment bounded by two membranes with unequal reflection coefficients could drive trans-compartmental water flow. They suggested that such a model might be applicable to epithelial transport but they declined to speculate on the anatomical locus of the "middle compartment." The Curran-MacIntosh model was analyzed in complete mathematical detail by Patlak, Goldstein and Hoffman (1963) who showed that qualitatively such an arrangement could accurately represent epithelial behavior. Whitlock and Wheeler (1964) reported that this analysis was in agreement with their data and proposed that the lateral intercellular space was the "middle compartment" bounded by lateral cell membrane and basement membrane.

Diamond (1964*b*) attempted to test this "double membrane effect" quantitatively. In a large series of experiments, rabbit gallbladders transported from 10–50% of their mucosal contents and then the ionic

composition of the transported fluid as well as that of the remaining mucosal contents was determined. Within 3 ‰, the tonicity of each solution was identical. With Diamond's estimates of the solute transport rate and cell water permeability, a simplified compartmental model predicted a grossly hypertonic reabsorbate when transporting between two equiosmolar media. It was felt that such results clearly disqualified the model.

Nevertheless, further work of Tormey and Diamond (1967) suggested that the lateral intercellular space was at least part of the route of transepithelial volume flow. In a companion paper to these observations, Diamond and Bossert (1967) suggested the "standing gradient hypothesis" as a means by which the lateral intercellular space could remain the locus of coupling of solute and solvent fluxes and still yield isotonic transport between equiosmolar media. In this model, the assumption of a well-stirred lateral intercellular compartment (channel) was discarded. Instead, solute entered the channel near its apex, creating local hypertonicity, which gradually equilibrated (via solvent influx across the lateral cell wall) as the channel contents flowed to the serosa. In this model, channel geometry was crucial. In one set of calculations, a channel radius of 0.1 micron yielded isotonic transport while for a radius of 1.0 micron the reabsorbate was grossly hypertonic. Using a linear approximation to the Diamond-Bossert differential equation, Segel (1970) was able to derive an analytical expression for the tonicity of standing gradient transport and showed that the significant geometric parameter in its determination was L^2/r where L is channel length and r channel radius.

A.E. Hill (1975*a*), however, raised serious objections to the standing gradient model. His solution of the Diamond-Bossert differential equation with "best guesses" for the parameters of several epithelia resulted in grossly hypertonic transport. Hill (1975*b*) considered the possibility of solvent flux across the tight junction into the lateral intercellular space, but again his calculations would not predict isotonic transport between equiosmolar bathing media. Diamond (1978) objected that Hill's parameter choices were wrong.

In contrast to the pessimistic calculations of Hill, Sackin and Boulpaep (1975) presented a detailed model of transport across *Necturus* proximal tubule claiming that both a standing gradient model and a compartment model were compatible with isotonic transport. With uniform solute input along the entire length of the channel, their continuous model predicted only small solute gradients within the intercellular space, and thus suggested that a compartment model would be adequate to represent this tissue. Indeed, for the *Necturus* proximal tubule (with a solute transport rate about one-tenth of Diamond's estimation for rabbit gallbladder) a compartment model predicted reabsorbtion between 1 % and 18 % hypertonic to the bathing media.

In a series of papers (Mikulecky, 1977; Mikulecky, Wiegand & Shiner, 1977; Mikulecky & Thomas, 1978), Mikulecky and co-workers have applied network thermodynamics to coupled flows across composite membrane systems and have also applied it to a model of salt and water flow across the kidney proximal tubule (Thomas & Mikulecky, 1978). Numerical solutions of the proximal tubular model were done using nonlinear circuit simulators. The authors state that the network method has many advantages over other approaches and say (Thomas & Mikulecky, 1978), "Compared with conventional compartmental analysis this approach can give solutions with fewer simplifying assumptions, requires only a simple circuit description in the language of the simulator on hand, easily handles nonlinear couplings of flows and forces, and suffers none of the shortcomings inherent in traditional 'electrical equivalent circuit' approach to compartmental flow problems."

In our own mathematical model of *Necturus* gallbladder (Weinstein & Stephenson, 1978, 1979) we found, in agreement with Sackin and Boulpaep, that concentration gradients along the length of the channel were relatively small. This reflected our choice of uniform solute pumps down the channel, as well as relatively wide intercellular spaces (about 10 % of cell volume) as reported by Spring and Hope (1978). We also noted average channel osmolality little different from bathing media osmolality. Qualitatively, the compartmental model gives results that are very similar to the distributed parameter model, although there may be significant quantitative differences between the predictions of the two models. This point is discussed in more detail elsewhere.[1] It was found, however, that with equiosmolar bathing media our model predicted a grossly hypertonic transported solution. The significance of this result was assessed by considering the numerical experiment in which mucosal bath salt concentration is varied while holding serosal concentration fixed. It was observed that as mucosal bath osmolality declined, the reabsorbate tonicity fell markedly. Indeed, within 1 % of bathing media isotonicity, transport was at equilibrium.

The importance of small degrees of mucosal hypotonicity as the driving force for transepithelial volume flow has been stressed by Andreoli and Schafer

[1] Weinstein, Alan M., and Stephenson, John L. Coupled water transport in standing gradient models of the lateral intercellular space (*Submitted for publication*)

(1978) and Andreoli, Schafer and Troutman (1978), in considerations of proximal tubule. They have argued that this very water-permeable epithelium in its normal functional state may be represented as a single membrane with parallel cellular and junctional elements. In this case, the middle compartment is absent from the model. Nevertheless, the role for transepithelial osmotic gradients in the transport of water across other tissues remains uncertain. In particular the problem remains of rationalizing apparently isotonic transport in the case of relatively low epithelial water permeability.

1. General Linear Theory of Epithelial Transport

Regardless of their complexity, and regardless of the phenomenology of membrane transport, models of epithelial transport determine the flows of solute and water across the epithelium as a function of the concentrations, pressures, and electrical potential of the bulk solutions bathing mucosal and serosal surfaces. If we restrict our attention to a single neutral solute we may write

$$J_s = J_s(C_M, C_S, P_M, P_S;\ C_0, P_0) \tag{1-1}$$

and

$$J_v = J_v(C_M, C_S, P_M, P_S;\ C_0, P_0) \tag{1-2}$$

where J_s is the net total transepithelial solute flux, J_v the net total volume flux, C_0 and P_0 are reference concentration and pressure, $C_0 + C_M$ and $P_0 + P_M$ are mucosal concentration and pressure, and $C_0 + C_S$ and $P_0 + P_S$ are serosal concentration and pressure.

If mucosal and serosal concentrations and pressures are restricted to a sufficiently small neighborhood of C_0 and P_0, we can expand J_s and J_v in a Taylor series and retain only linear terms to give

$$J_s = (J_s)_0 + \left[\frac{\partial J_s}{\partial C_M}\right]_0 C_M + \left[\frac{\partial J_s}{\partial C_S}\right]_0 C_S + \left[\frac{\partial J_s}{\partial P_M}\right]_0 P_M + \left[\frac{\partial J_s}{\partial P_S}\right] P_S \tag{1-3}$$

and

$$J_v = (J_v)_0 + \left[\frac{\partial J_v}{\partial C_M}\right]_0 C_M + \left[\frac{\partial J_v}{\partial C_S}\right]_0 C_S + \left[\frac{\partial J_v}{\partial P_M}\right]_0 P_M + \left[\frac{\partial J_v}{\partial P_S}\right] P_S. \tag{1-4}$$

Here $(J_s)_0$ and $(J_v)_0$ are solute and volume flows for $C_M = C_S = P_M = P_S = 0$, i.e., with equal mucosal and serosal bathing solutions. For the present, we will consider only variations in the concentrations. Thus near the reference state, the concentration of the transported solution is

$$C_R \equiv \frac{J_s}{J_v} = \frac{(J_s)_0 + \left[\frac{\partial J_s}{\partial C_M}\right]_0 C_M + \left[\frac{\partial J_s}{\partial C_S}\right]_0 C_S}{(J_v)_0 + \left[\frac{\partial J_v}{\partial C_M}\right]_0 C_M + \left[\frac{\partial J_v}{\partial C_S}\right]_0 C_S}. \tag{1-5}$$

For the particular case in which the fluxes respond in a symmetric manner to alterations in the bathing media

$$\frac{\partial J_s}{\partial C_M} = -\frac{\partial J_s}{\partial C_S} \quad \text{and} \quad \frac{\partial J_v}{\partial C_M} = -\frac{\partial J_v}{\partial C_S}$$

so that the above expression for C_R reduces to

$$C_R = \frac{(J_s)_0 + \left[\frac{\partial J_s}{\partial C_M}\right]_0 (C_M - C_S)}{(J_v)_0 + \left[\frac{\partial J_v}{\partial C_M}\right]_0 (C_M - C_S)}. \tag{1-6}$$

The reader should note that this assumption of symmetry is not carried through our subsequent analysis.

From the general development above we may consider the representation of the experimental situations that have been taken as indicative of "isotonic" transport. In one case a gallbladder with relatively small mucosal volume at concentration C_0 is placed in a large serosal bath also at C_0. The gallbladder is observed to transport a substantial fraction of its mucosal content into the serosal bath with only minimal deviation of C_M (Diamond, 1962; Whitlock & Wheeler, 1964). For this case we may assume that there is no change in the serosal concentration and that the mucosal bath is at a transport equilibrium. Thus, for C_M^* the limiting mucosal deviation

$$C_0 + C_M^* = C_R = \frac{(J_s)_0 + \left[\frac{\partial J_s}{\partial C_M}\right]_0 C_M^*}{(J_v)_0 + \left[\frac{\partial J_v}{\partial C_M}\right]_0 C_M^*}; \tag{1-7}$$

so that to first order (i.e., dropping terms in $(C_M^*)^2$)

$$C_M^* = -\frac{(J_s)_0 - C_0(J_v)_0}{-C_0\left[\frac{\partial J_v}{\partial C_M}\right]_0 + \left[\frac{\partial J_s}{\partial C_M}\right]_0 - (J_v)_0}. \tag{1-8}$$

In a second type of experiment, the gallbladder transports the reference solution from a relatively large muscosal bath into a small serosal bath and the osmolality of the serosal medium is measured. This is accomplished by freely suspending the gallbladder

and collecting the transported solution as drainage from the serosal surface (Diamond, 1964*b*; Hill & Hill, 1978*b*). With this preparation, the observation is made that the osmolality of the serosal medium differs little from the reference. Setting C_S^*, the steady-state serosal deviation from reference we may write

$$C_0 + C_S^* = C_R = \frac{(J_s)_0 + \left[\frac{\partial J_s}{\partial C_S}\right]_0 C_S^*}{(J_v)_0 + \left[\frac{\partial J_v}{\partial C_S}\right]_0 C_S^*}, \tag{1-9}$$

so that to first order

$$C_S^* = + \frac{(J_s)_0 - C_0(J_v)_0}{+ C_0\left[\frac{\partial J_v}{\partial C_S}\right]_0 - \left[\frac{\partial J_s}{\partial C_S}\right]_0 + (J_v)_0}. \tag{1-10}$$

When the fluxes respond in a symmetric manner to alterations in the bathing media C_S^* may be rewritten

$$C_S^* = \frac{(J_s)_0 - C_0(J_v)_0}{- C_0\left[\frac{\partial J_v}{\partial C_M}\right]_0 + \left[\frac{\partial J_s}{\partial C_M}\right]_0 + (J_v)_0}. \tag{1-11}$$

It may be concluded from these considerations that the verification that an epithelial model predicts isotonic transport involves the calculation of both C_M^* and C_S^* and the demonstration that both these deviations are only a small fraction of C_0. In practice, with models of the "isotonically" transporting epithelia, $C_M^* \approx - C_S^*$ and a useful estimate of these values is obtained by solving the equation

$$C_0 = C_R = \frac{(J_s)_0 + \left[\frac{\partial J_s}{\partial C_M}\right]_0 C^*}{(J_v)_0 + \left[\frac{\partial J_v}{\partial C_M}\right]_0 C^*}, \tag{1-12}$$

or

$$C^* = - \frac{(J_s)_0 - C_0(J_v)_0}{- C_0\left[\frac{\partial J_v}{\partial C_M}\right]_0 + \left[\frac{\partial J_s}{\partial C_M}\right]_0}. \tag{1-13}$$

This corresponds to the hypothetical experiment in which the mucosal osmolality is altered by an amount C^* to obtain a transported solution that is exactly at the reference concentration.

It must be stressed that the simple calculation of

$$(C_R)_0 = \frac{(J_s)_0}{(J_v)_0}, \tag{1-14}$$

the osmolality of the transported solution in the presence of exactly equal bathing media, may not be sufficient to decide whether an epithelial model will predict isotonic transport in the experimental setting. Nevertheless, $(C_R)_0$ is an important theoretical aspect of any epithelial model and provides a measure of the tightness of coupling of solute and solvent transport. It is, in fact, useful to define the coupling coefficient of osmotic transport (or coupling efficiency, as it is termed by Hill and Hill (1978*a*)) by

$$\gamma \equiv \frac{(J_v)_0}{(J_s)_0/C_0} = \frac{C_0}{(C_R)_0}. \tag{1-15}$$

Thus the coupling coefficient is the ratio of the actual volume flow to the virtual volume flow that would occur if reabsorption were "isotonic". Alternatively it is the ratio of the osmolality of the equal mucosal and serosal baths to the osmolality of the absorbate. The predicted deviations from isotonicity in the transport experiments may now be rewritten using this coupling coefficient as, for example,

$$C^* = \frac{-(J_s)_0(1-\gamma)}{- C_0\left[\frac{\partial J_v}{\partial C_M}\right]_0 + \left[\frac{\partial J_s}{\partial C_M}\right]_0}. \tag{1-16}$$

Hence, an epithelial model will predict isotonic transport when either coupling is tight ($(C_R)_0 \approx C_0$) or when $- C_0\left[\frac{\partial J_v}{\partial C_M}\right]_0 + \left[\frac{\partial J_s}{\partial C_M}\right]_0$ is large relative to $(J_s)_0$. This latter condition can be understood as a measure of epithelial permeability, as may be appreciated by examining transport across a simple membrane.

Consider a membrane for which fluxes are described by the Kedem and Katchalsky phenomenology

$$J_v = L_p[RT\sigma(C_S - C_M) + P_M - P_S] \tag{1-17}$$

and

$$J_s = N + J_v(1-\sigma)\,\bar{C} + H_s(C_M - C_S); \tag{1-18}$$

then

$$(J_v)_0 = 0, \quad (J_s)_0 = N, \tag{1-19}$$

$$\left[\frac{\partial J_v}{\partial C_M}\right]_0 = - \left[\frac{\partial J_v}{\partial C_S}\right]_0 = - L_p RT\sigma,$$

and

$$\left[\frac{\partial J_s}{\partial C_M}\right]_0 = - \left[\frac{\partial J_s}{\partial C_S}\right]_0 = - L_p RT\sigma(1-\sigma)\,C_0 + H_s, \tag{1-20}$$

implying

$$C_M^* = - C_S^* = C^* = \frac{-N}{L_p RT\sigma^2 C_0 + H_s}. \tag{1-21}$$

In the case of the single membrane, $\gamma=0$, so that the observation of small equilibrium osmotic deviations must result from either large hydraulic conductivity or a membrane solute permeability sufficiently large to preclude the development of substantial solute gradients.

The linearized form of the general transport equations [Eqs. (1-3) and (1-4)] may also be used to estimate the model predictions of transport of volume and solute against a potential gradient. The maximum concentration gradient against which the epithelium will transport solute is given by the solution of $J_s=0$, which under the linear approximation is

$$C_M=-(J_s)_0\Big/\left[\frac{\partial J_s}{\partial C_M}\right]_0. \tag{1-22}$$

Similarly, the maximum gradient against which it will transport water is given by the solution of $J_v=0$ or

$$C_M=-(J_v)_0\Big/\left[\frac{\partial J_v}{\partial C_M}\right]_0. \tag{1-23}$$

This we term the "strength of transport." Of course C_M, the deviation from the reference, may be substantial and the accuracy of this approximation cannot, in general, be guaranteed.

2. A Compartment Model of the Lateral Intercellular Space

In this section, we shall consider in detail the linearization (in concentration and pressure) of a single-solute compartment model of the lateral intercellular space. This linear approximate model will be used to verify the criteria of isotonic transport for the interspace model and to estimate the strength of transport. Further, it will also enable us to examine the influence of intraepithelial solute polarization effects on the measurement of tissue water permeability, that is to say, under what circumstances the effect of the channel basement membrane is significant. The numerical agreement with the nonlinear model equations is illustrated.

Consider an intercellular compartment (the channel) bordered by mucosal and serosal baths and by the cell (Fig. 1). All compartments contain a single salt solution; the osmolality and pressure in the serosal bath is denoted by C_0+C_S and P_0+P_S, in the channel by C_0+C_E, and P_0+P_E, and in both mucosal bath and cell by C_0+C_M and P_0+P_M, where C_0 is some fixed reference concentration. The mucosal bath may contain an impermeant species at osmolality C_i. The channel is bounded by apical (A), basal (B), and lateral (L) membranes. For each membrane there is an associated area A_α, water permeability $L_{P\alpha}$, reflection coefficient σ_α and solute permeability h_α, as well as transmural flux of volume, $J_{v\alpha}$, and solute, $J_{s\alpha}$, ($\alpha=A,B,L$). Across the lateral membrane there is solute transport into the channel at rate N.

Denoting $L_\alpha=A_\alpha L_{p\alpha}$ and $H_\alpha=A_\alpha h_\alpha$ we may write the standard Kedem-Katchalsky equations for volume flux

$$J_{vA}=L_A[(P_M-P_E)-RTC_i+RT\sigma_A(C_E-C_M)], \tag{2-1}$$
$$J_{vL}=L_L[(P_M-P_E)-RTC_i+RT\sigma_L(C_E-C_M)], \tag{2-2}$$
$$J_{vB}=L_B[(P_E-P_S)+RT\sigma_B(C_S-C_E)], \tag{2-3}$$

and for solute flux

$$J_{sA}=J_{vA}(1-\sigma_A)(C_0+\bar{C}_A)+H_A(C_M-C_E), \tag{2-4}$$
$$J_{sL}=N+J_{vL}(1-\sigma_L)(C_0+\bar{C}_A)+H_L(C_M-C_E), \tag{2-5}$$
$$J_{sB}=J_{vB}(1-\sigma_B)(C_0+\bar{C}_B)+H_B(C_E-C_S). \tag{2-6}$$

Here

$$C_0+\bar{C}_A=\frac{C_E-C_M}{\ln(C_0+C_E)-\ln(C_0+C_M)} \tag{2-7}$$

and

$$C_0+\bar{C}_B=\frac{C_E-C_S}{\ln(C_0+C_E)-\ln(C_0+C_S)} \tag{2-8}$$

are the mean osmolalities of the tight junction and basement membrane. The system of equations may be completed by specifying the two steady-state mass balance relations

$$J_{vB}=J_{vA}+J_{vL}, \tag{2-9}$$
$$J_{sB}=J_{sA}+J_{sL}.$$

These equations determine the intensive channel variables, P_E and C_E, as well as transepithelial volume flux, $J_v=J_{vB}$, and solute flux, $J_s=J_{sB}$, as functions of the independent variables P_M, C_M, P_S, C_S, C_i and N.

It may be observed that the only nonlinearity of the state variables in the model equations lies in the solvent drag term of the transmembrane solute fluxes. Furthermore, it is clear that if $P_M=P_S=C_M=C_S=C_i=N=0$, then $C_E=P_E=J_v=J_s=0$ is a solution to the system. It is natural, therefore, in an attempt to simplify the model, to linearize the model equations about this solution and consider the approximate solute flux relations:

$$J_{sA}=J_{vA}(1-\sigma_A)\,C_0+H_A(C_M-C_E), \tag{2-10}$$
$$J_{sL}=N+J_{vL}(1-\sigma_L)\,C_0+H_L(C_M-C_E), \tag{2-11}$$
$$J_{sB}=J_{vB}(1-\sigma_B)\,C_0+H_B(C_E-C_S). \tag{2-12}$$

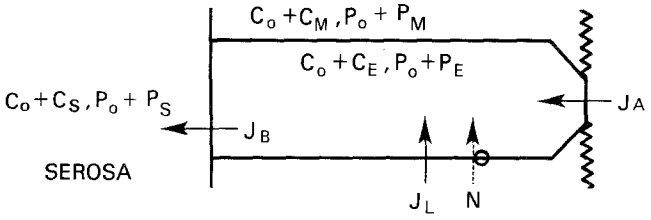

Fig. 1. Schematic representation of the lateral intercellular space. The cell and mucosal medium are assumed to be at the same osmolality and pressure

It may be noted that this linearization is an adaptation to a compartment model of the "isotonic convection approximation" introduced by Segel for the analysis of the continuous channel model (Segel, 1970; Lin & Segal, 1974).

The analytical solution of the linear model equations may be fruitfully approached in two stages: In Case I, it is assumed that flux across the tight junction is negligible and that there is no diffusion across the lateral cell membrane – this defines an elementary model much like that discussed by Diamond (1964*b*) but for the inclusion of a basement membrane with finite solute permeability. In Case II, it will be seen how the inclusion of a permeable tight junction may modify the behavior predicted by the elementary model.

Case I: Sealed Tight Junction

When there is insignificant junctional flux, the equations of mass balance take the form

$$J_v = L_B(P_E - P_S) = L_L[(P_M - P_E) - RTC_i + RT(C_E - C_M)], \tag{2-13}$$

$$J_s = L_B(P_E - P_S)\,C_0 + H_B(C_E - C_S) = N, \tag{2-14}$$

which may be solved for P_E and C_E. Setting $L_{LB} = \frac{L_L L_B}{L_L + L_B}$,

$$C_E = \frac{1}{H_B + RTL_{LB}C_0}[N + H_B C_S + L_{LB}C_0 \cdot (P_S - P_M + RTC_i + RTC_M)], \tag{2-15}$$

and the transepithelial fluxes are found to be

$$J_v = \frac{L_{LB}H_B}{H_B + RTL_{LB}C_0}\left[P_M - P_S + \frac{RTN}{H_B} - RTC_i + RT(C_S - C_M)\right], \tag{2-16}$$

$$J_s = N. \tag{2-17}$$

From these expressions certain global parameters of transport may be determined; namely: the hydraulic conductivity of the epithelium

$$L_p = \frac{L_{LB}H_B}{H_B + RTL_{LB}C_0}; \tag{2-18}$$

the tonicity of the fluid transported between equal bathing media

$$(C_R)_0 = \frac{H_B}{RTL_p} = C_0 + \frac{H_B}{RTL_{LB}}; \tag{2-19}$$

the osmotic coupling coefficient

$$\gamma = \frac{C_0}{(C_R)_0} = \frac{RTL_{LB}C_0}{H_B + RTL_{LB}C_0} = 1 - \frac{L_p}{L_{LB}}; \tag{2-20}$$

the osmotic deviations necessary to assess isotonicity of transport

$$C_M^* = \frac{-N}{L_{LB}RT(C_0 - N/H_B)}, \tag{2-21}$$

$$C_S^* = \frac{N}{L_{LB}RT(C_0 + N/H_B)}, \tag{2-22}$$

and

$$C^* = \frac{N}{L_{LB}RTC_0}; \tag{2-23}$$

and finally the maximum osmotic gradient against which volume can be transported

$$\hat{C} = \frac{N}{H_B}. \tag{2-24}$$

(This maximum gradient, $\hat{C}$, is precisely that specified in Eq. (1-23).)

In the case of the continuous channel model, a considerable amount of attention has been given to the calculation of the tonicity of the fluid transported between equal bathing media (Diamond & Bossert, 1967; Segel, 1970; Hill, 1975*a*; Sackin & Boulpaep, 1975). As in the continuous case, the linear analysis of the elementary compartment model shows the reabsorbate tonicity, $(C_R)_0$, to be independent of the transport rate, N. For basement membrane electrical resistance either 10 Ωcm^2 (Henim, Cremaschi, Schettino, Meyer, Donin & Cotelli, 1977) or 1 Ωcm^2 (suggested by the observation of Wright and Diamond (1968)) the tonicity of the fluid transported between equal bathing media, $(C_R)_0$, is tabulated for a range of lateral membrane water permeabilities in Table 1. In these calculations $C_0 = 0.2$ mOsm/cm^3 and basement membrane water permeability, $L_B = 0.5 \times$

Table 1. $(C_R)_0$ (mOsm/liter)

Ω (ohm cm^2)	H_B[a] (cm/sec)	L_L (cm^3/sec mmHg cm^2 epithelium)				
		10^{-9}	10^{-8}	10^{-7}	10^{-6}	10^{-5}
1	1.25×10^{-3}	66,003	6,792	871	279	220
10	1.25×10^{-4}	6,780	859	267	208	202

[a] For solute permeability H(cm/sec), the ion flow across a membrane is given by the relation

$$I = HA\bar{C}\frac{(zF)^2}{RT}\Delta\psi,$$

where I is the current carried by the species (amp), A is membrane area (cm^2), $zF = 10^5$ Coul/mol, $RT = 2.5\times10^3$ Joul/mol, $\bar{C}$ is mean ion concentration (mol/cm^3) and $\Delta\psi$ is transmembrane potential (volt). Thus, the membrane resistance, Ω (ohm cm^2), is given by

$$\Omega = \frac{\Delta\psi}{I}\cdot A = \frac{1}{H}\frac{RT}{\bar{C}(zF)^2} = \frac{1.25\times10^{-3}}{H}$$

for a mean ion concentration $\bar{C}\approx0.2\times10^{-3}$ mol/cm^3.

10^{-5} cm^3/sec mmHg. (L_B reflects the permeability of the basement membrane material, 10^{-4} cm/sec mmHg (Welling & Grantham, 1972), as well as an estimated 5% of epithelial area occupied by the channel mouth.)

It is clear that only for values of L_L at least several times greater than have been reported for the very permeable rabbit proximal rubule (3.5×10^{-7} cm^3/secmmHg by Andreoli et al. (1978)) is C_R nearly isotonic to the bathing media. Thus, in agreement with Hill (1975*a*), the computed values of $(C_R)_0$ are quite high. It must be emphasized, however, that the experimental determination of $(C_R)_0$ would involve fixing each bathing medium at the reference osmolality and making independent measurements of both transepithelial salt and water fluxes.

The model requirements for isotonic transport may be appreciated from an examination of the parameter dependence of C^*, the deviation of the mucosal bath concentration from the reference at which the reabsorbate tonicity equals the reference tonicity. It may be noted that in the compartment model when the reabsorbate tonicity is equal to the reference tonicity ($C_R = C_0$) the channel itself is isotonic to the serosa ($C_E = 0$). Since in this case there is no solute diffusion across the basement membrane it is reasonable that C^* is, in fact, independent of H_B. On the other hand, C^* is linearly dependent upon the tissue transport rate. For $N = 0.5\times10^{-6}$ mOsm/sec cm^2, as in *Necturus* gallbladder (Spring & Hope, 1979*a*) or $N = 4.0\times10^{-6}$ mOsm/seccm^2 as in rabbit gallbladder (Diamond, 1964*a*) the predicted values of C^* from the elementary compartment model are indicated in Table 2 for a range of lateral

Table 2. C^* (mOsm/liter)

N (mOsm/sec cm^2)	L_L (cm^3/sec mmHg cm^2 epithelium)				
	10^{-9}	10^{-8}	10^{-7}	10^{-6}	10^{-5}
0.5×10^{-6}	130	13	1.3	0.16	0.039
4.0×10^{-6}	1100	110	11.0	1.30	0.32

membrane water permeabilities ($L_B = 0.5\times10^{-5}$ cm^3/secmmHg. $C_0 = 0.2$). The tabulated values of C^* show that in *Necturus*, isotonicity of bathing solutions would be observed for $L_L > 2\times10^{-8}$ and in the rabbit for $L_L > 2\times10^{-7}$. These values of L_L may be viewed in light of the unit membrane water permeability, 1.2×10^{-8} cm/secmmHg, determined in the red cell by Sha'afi, Rich, Sidel, Bossert and Solomon (1967). L_L is however the product of this unit permeability and the ratio of lateral cell membrane area to epithelial area. This membrane area ratio may be substantially greater than one, as, for example, in rabbit proximal nephron where Welling and Welling (1975) have found it to be 20 cm^2/cm^2 epithelium in convoluted tubule and 10 cm^2/cm^2 epithelium in straight tubule.

Hill (1977) has used numerical solution of the continuous channel model to investigate the serosal-mucosal osmolality difference in the case that the serosal medium is created by the gallbladder reabsorbate. (In the continuous model this corresponds to the boundary condition $dC/dx|_{x=L} = 0$.) His graphical display of results for $N = 0.6\times10^{-6}$ mOsm/seccm^2 (Fig. 4, Hill, 1977) appears to be compatible with the values of Table 2, line 1. In discussing his results, however, Hill felt that in the simulation of the unilateral preparation with very hypotonic luminal contents, the model predicted an unacceptably high discrepancy between the bathing media. Similarly, in the elementary compartment model

$$\frac{C^*}{C_0} = \frac{-N}{RTL_{LB}C_0^2}$$ may get quite large for small C_0.

Nevertheless, in a hypotonic environment it is entirely plausible that L_L may increase, reflecting perhaps, increased membrane hydration. Put conversely, it seems unlikely that L_L should be completely independent of the reference state and the possibility of this dependence has been alluded to by Hill in subsequent discussions (Hill & Hill, 1978*b*). Indeed Diamond (1966) has presented evidence suggesting that cell membrane water permeability may vary inversely with the mean tonicity of the bathing solutions.

It is of interest to reconsider Diamond's early analysis of the elementary compartment model (1964*b*). Given equal bathing media at osmolality O_0, the tonicity of the transported fluid, C, was found to be

$$C=\frac{O_0}{2}\left[1+\sqrt{1+\frac{4N}{RTL_{LB}O_0^2}}\right]. \tag{2-25}$$

However, in deriving this expression the assumption was made that there was no diffusive loss of solute from the channel across the basement membrane. As has been shown above, this implicitly introduces into the calculation the assumption that (1) the channel and serosa are at equal osmolality, C_0, and (2) the mucosal osmolality is in fact somewhat less than the serosa and is given by C_0+C^*. Repeating Diamond's analysis with the explicit incorporation of the underlying assumptions yields the relation

$$C_0=\left(\frac{C_0+C^*}{2}\right)\left[1+\sqrt{1+\frac{4N}{RTL_{LB}(C_0+C^*)^2}}\right], \tag{2-26}$$

which has the exact solution $C^*=\dfrac{-N}{RTL_{LB}C_0}$. Hence, when O_0 in the Diamond formula is taken as the tonicity of the mucosal contents of the gallbladder, the computed concentration, C, is indeed the osmolality of the serosal drainage in the unilateral preparation (an observation also made by Hill, 1977).

Thus, for the compartment model of the interspace transporting at quasi-steady state there appears to be little role for solute trapping within the interspace to enhance the transepithelial flow of water. The model behaves as though it were a simple membrane with hydraulic conductivity, L_{LB} and the driving force for solvent flow just luminal hypotonicity. Andreoli and co-workers have emphasized the point that for the highly water permeable proximal convoluted tubule (Andreoli et al., 1978) and *pars recta* (Andreoli & Schafer, 1978) small values of C^* (experimentally indistinguishable from zero) suffice to account for observed water flows.

In contrast, however, the large water flows across the vigorously transporting rabbit gallbladder have been more difficult to understand in light of the lower water permeability of this tissue. Although standing gradient theory offered a potential resolution to this difficulty, calculations using the channel dimensions of actively transporting epithelia have not shown significant gradients (Hill, 1975*a*). It remained, therefore, to reexamine the accuracy of what was thought to be the water permeability relevant to the model. Diamond's discussion (1978) of the data of Wright, Smulders and Tormey (1972) stressed the fact that the 30-min determination of water permeability (3×10^{-9} cm/secmmHg) was substantially less than that calculated from the flows during the first five minutes of the experiment (3×10^{-8} cm/sec mmHg). The cause of the slow decline in water flow during the L_p determination was not apparent; intraepithelial solute polarization should theoretically be complete within seconds (Diamond, 1978; Weinstein & Stephenson, *unpublished*). Diamond speculated that the effects of solute polarization within the channel might well mask another order of magnitude increment in the cell membrane water permeability. In fact, the effects of such polarization on the steady state water permeability determination are predicted by the elementary compartment model and are realized as the effect of H_B on the calculated L_p.

Table 3. $L_p\times10^8$ cm^3/sec mmHg cm^2 epithelium

Ω (ohm cm^2)	H_B (cm/sec)	L_L (cm^3/sec mmHg cm^2 epithelium)				
		10^{-9}	10^{-8}	10^{-7}	10^{-6}	10^{-5}
1	1.25×10^{-3}	0.1	0.96	7.6	24.	30.
10	1.25×10^{-4}	0.097	0.77	2.5	3.2	3.3
100	1.25×10^{-5}	0.077	0.25	0.32	0.33	0.33

Table 3 shows the dependence of tissue L_p on both the basement membrane solute permeability and the cell membrane water permeability ($C_0=$ 0.2 mOsm/cm^3, $L_B=0.5\times10^{-5}$ cm^3/sec mmHg). It should be observed that for increasing cell membrane water permeability solute entrapment plays a greater role in determining the epithelial hydraulic conductivity; at lower lateral membrane water permeabilities this role is manifest for the lower basement membrane solute permeabilities. In particular, for a basement membrane resistance for rabbit gallbladder 10 Ωcm^2 the 5-min L_p of Wright et al. (1972) is the maximum L_p observable for a steady-state experiment. L_L could be any value greater than 10^{-7} cm^3/sec mmHg and C^* might well be quite small. In this regard, it is of interest to note that if proximal tubule basement membrane resistance is 1 Ωcm^2, then the maximum observable steady-state L_p is 3×10^{-7} cm/sec mmHg, approximately the value reported by Andreoli et al. (1978). Indeed, Thomas and Mikulecky (1978) in their computer simulation of rat proximal tubule, have suggested the presence of substantial intraepithelial solute polarization effects. Finally, Hill and Hill (1978*b*) reported a hydraulic conductivity for ouabain-treated *Necturus* gallbladder of 9×10^{-9} cm/sec mmHg using direct application of hydrostatic pressure in a unilateral sac preparation. It is known, however, that ouabain treatment will increase the electrical resistance of proximal tubule (Lutz,

Cardinal & Burg, 1973) and the observations of Spring and Hope (1979*b*) on *Necturus* gallbladder suggest that this increase in electrical resistance occurs in association with a swelling of the cell and loss of cross-sectional area of the lateral interspace. It may be seen from the elementary compartment model that a decrease in interspace basement membrane area sufficient to increase basement membrane resistance to 30 Ωcm^2 will limit the gallbladder L_p to 9×10^{-9} cm/sec mmHg.

Case II: Permeable Tight Junction

The case of a permeable tight junction is approached by first considering the junction and lateral cell membrane as two parallel elements comprising the mucosal boundary of the channel. Setting

$$L_M = L_L + L_A, \tag{2-27}$$

$$\sigma_M = \frac{L_L\sigma_L + L_A\sigma_A}{L_L + L_A}, \tag{2-28}$$

$$H_M = H_A + H_L + (\sigma_L - \sigma_A)^2 RTC_0 \frac{L_A L_L}{L_A + L_L}; \tag{2-29}$$

the transmucosal fluxes are found to be

$$J_{vM} = J_{vA} + J_{vL} = L_M[P_M - P_E - RTC_i + RT\sigma_M(C_E - C_M)], \tag{2-30}$$

$$J_{sM} = J_{sA} + J_{sL} = J_{vM}(1-\sigma_M)C_0 + H_M(C_M - C_E) + N. \tag{2-31}$$

We may next analyze this composite mucosal membrane in series with the basement membrane. Denoting

$$L_{MB} = \frac{L_M L_B}{L_M + L_B}, \tag{2-32}$$

$$L_p = \frac{L_{MB}(H_M + H_B)}{H_M + H_B + RTL_{MB}(\sigma_M - \sigma_B)^2 C_0}, \tag{2-33}$$

$$\sigma = \frac{H_B\sigma_M + H_M\sigma_B}{H_B + H_M}, \tag{2-34}$$

$$H = \frac{H_M H_B}{H_M + H_B}, \tag{2-35}$$

the transepithelial fluxes may be written in terms of the transepithelial driving forces

$$J_v = L_p[P_M - P_S - RTC_i + RT\sigma\hat{C} + RT\sigma(C_S - C_M)], \tag{2-36}$$

$$J_s = J_v(1-\sigma)C_0 + H(C_M - C_S) + \frac{H_B N}{H_M + H_B}, \tag{2-37}$$

where

$$\hat{C} = \frac{(\sigma_M - \sigma_B)N}{H_B\sigma_M + H_M\sigma_B} \tag{2-38}$$

Table 4. Parameters for two hypothetical epithelia

	"Rabbit gallbladder"	"*Necturus* gallbladder"
Elementary parameters		
N [a]	4.0×10^{-6}	0.5×10^{-6}
L_B [b]	5.0×10^{-6}	5.0×10^{-6}
H_B [c]	1.25×10^{-4}	2.5×10^{-4}
σ_B	0.0	0.0
L_L	5.0×10^{-7}	0.5×10^{-7}
H_L	6.25×10^{-6}	0.0
σ_L	1.0	1.0
L_A	5.0×10^{-7}	0.5×10^{-7}
H_A	6.25×10^{-6}	6.25×10^{-6}
σ_A	0.9	0.7
Composite Parameters		
L_M	1.0×10^{-6}	1.0×10^{-7}
H_M	2.2×10^{-5}	1.5×10^{-5}
σ_M	0.95	0.85
L_{MB}	8.3×10^{-7}	9.8×10^{-8}
L_p	4.1×10^{-8}	4.9×10^{-8}
H	1.9×10^{-5}	1.4×10^{-5}
σ	0.81	0.80
Derived quantities		
$\hat{C}$ [d]	32.0	2.0
$(J_v)_0$ [e]	1.99×10^{-5}	1.47×10^{-6}
$(J_s)_0$ [f]	4.16×10^{-6}	5.30×10^{-7}
$(C_R)_0$	209.0	362.0
γ	0.96	0.55
$\left[\frac{dJ_v}{dC_M}\right]_0$	-6.21×10^{-4}	-7.33×10^{-4}
$\left[\frac{dJ_s}{dC_M}\right]_0$	-4.60×10^{-6}	-1.53×10^{-5}
C_M^*	−1.82	−1.83
C^*	−1.52	−1.81
C_S^*	1.30	1.79

[a] mmol/sec cm^2 epithelium.
[b] Water permeabilities (cm^3/sec mmHg cm^2 epithelium).
[c] Solute permeabilities (cm^3/sec cm^2 epithelium).
[d] Concentrations (mmol/liter).
[e] Volume flux (ml/sec cm^2 epithelium).
[f] Solute flux (mmol/sec cm^2 epithelium).

has the dimension of concentration and is the effective force for volume flow due to active salt transport. Again for equal bathing media

$$(J_v)_0 = RTL_p\sigma\hat{C} = RTL_p\frac{(\sigma_M - \sigma_B)N}{H_M + H_B}, \tag{2-39}$$

$$(J_s)_0 = (1-\sigma)C_0(J_v)_0 + \frac{H_B N}{H_M + H_B}, \tag{2-40}$$

$$(C_R)_0 = (1-\sigma)C_0 + \frac{H_B}{RTL_p(\sigma_M - \sigma_B)} = (1-\sigma_B)C_0 + \frac{H_B}{RTL_{MB}(\sigma_M - \sigma_B)}; \tag{2-41}$$

and the derivatives at the reference state,

$$-\left[\frac{\partial J_v}{\partial C_S}\right]_0 = \left[\frac{\partial J_v}{\partial C_M}\right]_0 = -RTL_p\sigma, \tag{2-42}$$

$$-\left[\frac{\partial J_s}{\partial C_S}\right]_0 = \left[\frac{\partial J_s}{\partial C_M}\right]_0 = RTL_pC_0(\sigma^2-\sigma)+H. \tag{2-43}$$

Thus, the mucosal osmotic deviation for steady-state transport may be written

$$C_M^* = \frac{RTL_p\sigma^2 C_0\hat{C} - \dfrac{H_B N}{H_M+H_B}}{RTL_p\sigma^2 C_0 + H - RTL_p\sigma\hat{C}}. \tag{2-44}$$

The introduction of a permeable tight junction permits the appearance of complex phenomena peculiar to composite membranes. Thus, even for $\sigma_A=1$, if, for example, the mucosal salt permeability is one-fourth that of the basement membrane, then a whole epithelial reflection coefficient of 0.8 will be measured. If $\sigma_A<1$ and both L_A and L_L are substantial then convective flow through the junction (and back across the lateral cell membrane) may give the impression of enhanced mucosal solute permeability. The latter phenomenon, namely $H_M>H_A+H_L$, allows, at least theoretically, for the calculation of the relative magnitude of junctional and lateral cell membrane water permeability. A prerequisite for this determination is that the whole epithelial parameters, L_p, H and σ, the basement membrane parameters, L_B, H_B and σ_B, as well as σ_L, H_L and H_A, be known. Then, using the defining relations for the composite permeabilities one may show

$$\frac{L_A}{L_L} = \frac{(\sigma_L-\sigma_M)^2 RTL_M C_0}{H_M-H_A-H_L}, \tag{2-45}$$

where the right-hand side is determined from

$$H_M = \frac{HH_B}{H_B-H}, \tag{2-46}$$

$$\sigma_M = \frac{H_B\sigma - H\sigma_B}{H_B-H}, \tag{2-47}$$

$$L_M = \frac{L_BL_p(H_B-H)}{(L_B-L_p)(H_B-H)-RT(\sigma-\sigma_B)^2 L_BL_pC_0}. \tag{2-48}$$

We shall gain a sense of the accuracy or range of utility of the isotonic convection approximation by comparing the numerical predictions of the linearized and nonlinear models for two hypothetical epithelia in several steady-state experiments. Table 4 lists the individual and composite parameters for these epithelia, one with transport activity akin to rabbit gallbladder, the other to *Necturus* gallbladder.

It may be noted that the rabbit epithelium transports solute at eight times the rate of *Necturus*, so that with half the basement membrane solute permeability, the strength of this rabbit channel pump, $\hat{C}$, is 32 mOsm/liter (compared with 2 mOsm/liter for *Necturus*). Nevertheless, the water permeabilities have been so chosen that for either epithelium in a unilateral sac preparation the tonicity of the reabsorbed fluid will be 0.2 mOsm/cm^3 when the mucosal contents are within 1% of this value. It is of interest to observe that although the composite mucosal barrier for the rabbit is an order of magnitude more water permeable than in *Necturus*, the two models have comparable whole epithelial hydraulic conductivities, due to solute polarization effects.

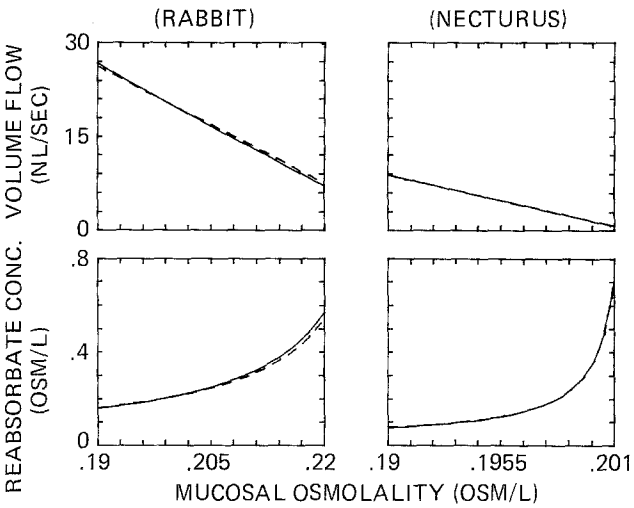

Fig. 2. Comparison of the channel model and its linearization. For both the rabbit and *Necturus* parameter sets volume flow (J_v) and reabsorbate concentration ($C_R=J_s/J_v$) are graphed as mucosal salt concentration is varied. (Serosal salt concentration is fixed at 0.2 Osm/liter.) Solution to the nonlinear equations is plotted as solid curves, to the linear model as dashed curves. With the *Necturus* parameters, the two models result in virtually identical predictions

Fig. 2 shows the simulation of steady-state experiments in which the epithelium is placed between media of fixed concentration. In each case, both baths are of equal pressure, there are no impermeant species present and the serosal bath is at 0.2 mOsm/cm^3. The effect on transport of varying mucosal bath salt concentration about 0.2 mOsm/cm^3 is displayed by plotting both J_v and J_s/J_v as a function of mucosal tonicity. (Variation in J_s is, in fact, relatively minor in these experiments.) For both the rabbit and *Necturus* parameters the predictions of the nonlinear models are indicated by solid curves and serve as a check on the predictions of the linear approximate models (dashed curves). It is clear that for the more sluggishly transporting *Necturus*, the accuracy of the approximation is a bit better. Nevertheless, it may be said for either epithelium that near $C_M=0$ the variation in J_v is accurately predicted. Thus, the epithelial

L_p estimated by the linear model should be close to that derived from the nonlinear model by computing numerically the derivative $L_p = \partial J_v / \partial C_i$. It is of interest to note that in the weakly transporting *Necturus*, near $C_M = 0$, small variations in C_M may produce large changes in the tonicity of the reabsorbate. Thus, although the *Necturus* model predicts isotonicity for any unilateral preparation, the model also predicts that separate solute and solvent flux measurements between large equal bathing media may show a ratio much greater than isotonicity.

A discrepancy with the experimental literature may be perceived in the inability of the rabbit model to transport volume against an adverse salt gradient of more than 32 mOsm/liter. The observations of Whitlock and Wheeler (1964) and Diamond (1964*a*) demonstrate that the rabbit gallbladder can, in fact, transport water against 40 mOsm/liter at a substantial fraction of the level flow rate. Within the framework of a Curran-MacIntosh type of epithelial model, weakness in transporting water against an osmotic gradient suggests inadequate hyperosmolality of the middle compartment. In terms of the linear approximate model, it means that the term $\sigma \hat{C} = \frac{\sigma_M N}{H_M + H_B}$ is too small, which, in turn, implies that H_B is too large. Yet in the model of the isotonically transporting rabbit gallbladder there is no experimental justification for choosing a basement membrane permeability smaller than 1.25×10^{-4} cm/sec.

We are led therefore to the supposition that in the placement of a hypertonic solution within the mucosal bath, the model parameters have changed from the level flow state. Indeed, Reuss and Finn (1977) have shown that in *Necturus* gallbladder, imposition of mucosal sucrose produces substantial increase in the electrical resistance of the lateral intercellular space. In the rabbit gallbladder, Smulders, Tormey and Wright (1972) have documented a 70% decline in lateral interspace area with the addition of 50 mOsm/liter sucrose to the mucosal bath. Thus, it appears that with the imposition of the osmotic gradient there is indeed a decrease in H_B that occurs in association with an appreciable loss of interspace area.

It seems reasonable to suppose that in these experiments, changes in channel dimensions are mediated by changes in channel pressure. For *Necturus* gallbladder between equal bathing media, Spring and Hope (1979*a*) have shown channel volume to be a sensitive function of changes in serosal pressure. To illustrate the possible role of channel pressure in modulating epithelial water transport we shall consider a simple compliance relation of the form

$$\frac{A_B}{A_B^0} = 1 + \mu (P_E - P_E^0), \tag{2-49}$$

where A_B is channel basement membrane area, P_E is channel pressure, and μ is a compliance constant. (A_B^0 and P_E^0 are area and pressure at level flow.) An alternative empirical compliance relation has been utilized by Huss and Marsh (1975) and Huss and Stephenson (1979) in their models of proximal tubule in which channel area is related to channel pressure through an exponential function. Nevertheless, over a wide range of serosal pressures the linear compliance law has been shown to give an adequate simulation of the changes in channel dimensions (Weinstein & Stephenson, 1979).

These compliance relations have been incorporated into the nonlinear channel model with the proportions

$$\frac{L_B}{L_B^0} = \frac{H_B}{H_B^0} = \frac{A_B}{A_B^0}. \tag{2-50}$$

(The rigid model is restored by setting $\mu = 0$.) Using the parameters for rabbit gallbladder and $\mu = 0.2/\text{mmHg}$[2], we have computed the transepithelial fluxes for both rigid and compliant models over a range of hypertonic mucosal bath concentrations. In Fig. 3, transepithelial volume flow (nl/sec cm^2) is plotted against mucosal salt concentration ranging from 200 to 280 mOsm/liter (with serosa at 200 mOsm/liter). Over this range the volume flow predicted by the rigid model is a linear function of concentration, with volume flow reversal occurring at a 32 mOsm/liter salt gradient. By contrast, the compliant model is still transporting at 25% of its level-flow rate against a salt gradient of 40 mOsm/liter and flow remains positive through 80 mOsm/liter. The insert is a graph of channel cross-section area (relative to the level flow area) as predicted by the compliant model for these same experiments. At the 80 mOsm/liter gradient, channel basement membrane area (and hence permeability) has decreased to approximately one-third its value at level flow.

Thus, the effect of incorporating a compliant lateral intercellular space into the channel model appears to be an enhanced capability of simulating water transport against an osmotic gradient while maintaining the desired level flow model characteristics. This last calculation is an example of a series of experiments for which the epithelial representation as a single membrane or as a rigid composite membrane is not adequate. Nevertheless, the compartment concept remains intact and steady-state experiments could still be simulated with a rigid interspace model although the appropriate parameter set might vary with the experimental conditions.

---

[2] In *Necturus* gallbladder, the data of Spring and Hope (1979*a*) indicate a value $\frac{1}{V_{Ch}} \frac{\partial V_{Ch}}{\partial P_S}\Big|_{P_S = 0} = 0.2/\text{mmHg}$, where V_{Ch} is channel volume and P_S is serosal pressure.

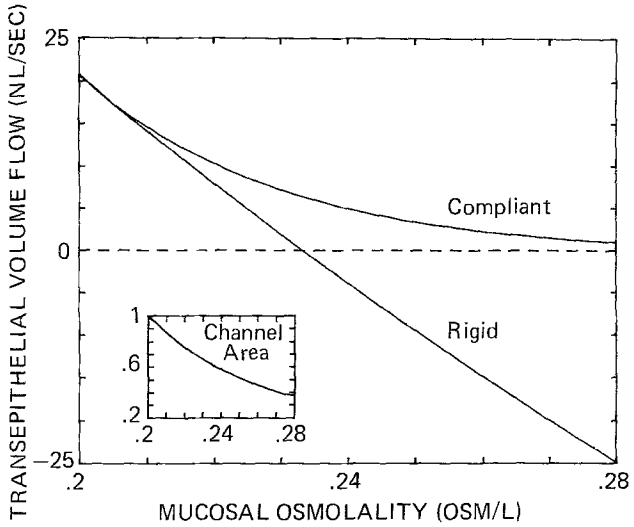

Fig. 3. Volume transport against an adverse osmotic gradient: Comparison of rigid and compliant models. Using the nonlinear channel model with the rabbit parameter set, transepithelial volume flow is determined as a function of mucosal salt concentration. (Serosa is fixed at 0.2 Osm/liter.) With a model of fixed geometry, volume flow remains a linear function of salt gradient and flow reversal occurs at 32 mOsm/liter. When the channel is permitted to collapse as channel pressure falls, the strength of transport is increased. Channel cross-section (relative to the level flow state) is shown in the insert

3. Application to a Comprehensive Epithelial Model

In this section we illustrate the use of the general analytical principles of Sect. 1, as well as the insight gained from the compartmental analysis, to understand the behavior of a comprehensive epithelial simulation. The model used for these calculations has previously been reported in detail (Weinstein & Stephenson, 1979) when it was used for the simulation of *Necturus* gallbladder epithelium. Here we shall also make use of another parameter set representing a more actively transporting epithelium, perhaps akin to rabbit gallbladder.

Briefly, the model consists of a cell and paracellular channel between well-stirred mucosal and serosal bathing media (Fig. 4). Variables of the model include electrical potential, hydrostatic pressure, and the concentrations of sodium, potassium, and chloride ions, as well as volume flow and the fluxes of the several solutes. In addition, the cell contains a negatively charged impermeant species. The cell actively extrudes sodium into the lateral intercellular space at a rate proportional to the intracellular sodium concentration, and potassium is taken up at the lateral membrane at a rate proportional to the sodium transport. There is coupled Na-Cl entry into the cell across the apical membrane.

Within both cell and channel, all variables are functions of position x, where $x=0$ just interior to the apical membrane or tight junction and $x=L$ at the basal or basement membranes. Mass conservation is represented by the steady-state equations

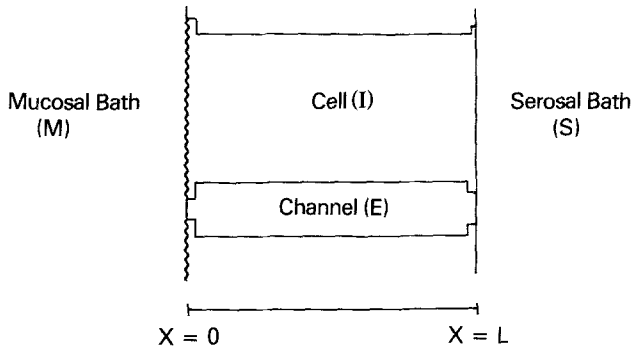

Fig. 4. Representation of cell and channel between mucosal and serosal bathing media. Except for tapering near the junction and basement membrane, the channel is assumed to be of uniform area

$$\frac{dF_{v\alpha}}{dx}(x)=J_{v\alpha}(x), \tag{3-1}$$

$$\frac{dF_{k\alpha}}{dx}(i,x)=J_{k\alpha}(i,x), \tag{3-2}$$

where $F_{v\alpha}$ and $F_{k\alpha}$ refer to axial volume and solute flows in compartment α ($\alpha=I$ or E, indicating cell or channel), i references the solute species, and J indicates flux across the lateral cell membrane into compartment α. The transmural fluxes J are given by the Kedem-Katchalsky relations for membranes so that, for example, flux into the channel is of the form

$$J_{vE}(x)=S\cdot L_{pIE}\cdot\{P_I(x)-P_E(x)-RT\Pi + RT\sum_i \sigma_{IE}(i)[C_E(i,x)-C_I(i,x)]\}, \tag{3-3}$$

$$J_{kE}(i,x)=J_{vE}(x)[1-\sigma_{IE}(i)]\,\bar{C}_{IE}(i,x)+NSP(i) + S\cdot h_{IE}(i)\cdot\{[C_I(i,x)-C_E(i,x)] + \bar{C}_{IE}(i,x)\frac{z(i)F}{RT}[\psi_I(x)-\psi_E(x)]\}, \tag{3-4}$$

with

$$\bar{C}_{IE}(i,x)=\frac{C_I(i,x)-C_E(i,x)}{\log(C_I(i,x))-\log(C_E(i,x))}, \tag{3-5}$$

where $P_\alpha(x)$, $\psi_\alpha(x)$, and $C_\alpha(i,x)$ are pressure, voltage and concentration in compartment α, Π is cell impermeant anion concentration, S is circumferential length of the cell-channel boundary, L_{pIE}, $\sigma_{IE}(i)$, and $h_{IE}(i)$ are water permeability, reflection coefficient, and solute permeability, NSP is an active transport term, $z(i)$ is solute valence, and R, T, F are gas constant, temperature, and the Faraday.

Further, it is assumed that within cell and channel the variables satisfy the Poiseuille equation

$$\frac{dP_\alpha}{dx}(x) = -\frac{8\pi\eta_\alpha}{A_\alpha^2(x)} F_{v\alpha}(x) \tag{3-6}$$

and the Nernst-Planck equation

$$F_{k\alpha}(i,x) = F_{v\alpha}(x)\, C_\alpha(i,x) - D_\alpha(i) A_\alpha(x) \frac{dC_\alpha}{dx}(i,x), \tag{3-7}$$
$$- u_\alpha(i)\, A_\alpha(x)\, C_\alpha(i,x) \frac{d\psi_\alpha}{dx}(x)$$

where A_α is cross-sectional area, η_α is viscosity and D_α and u_α are the appropriate mobilities. Electroneutrality demands

$$\begin{aligned} 0 &= \sum z(i)\, C_E(i,x), \\ 0 &= z_\pi \Pi + \sum z(i)\, C_I(i,x), \end{aligned} \tag{3-8}$$

where z_π is the mean valence of the impermeant anions.

The boundary conditions for this system of equations are specified implicitly by the transport laws at each of the bounding membranes. Thus, for example, at the channel basement membrane we require

$$F_{vE}(L) = A_{ES} L_{pES} \{P_E(L) - P_S + RT \sum_i \sigma_{ES}(i)[C_S(i) - C_E(i,L)]\}, \tag{3-9}$$

and

$$F_{kE}(i,L) = F_{vE}(L)[1-\sigma_{ES}(i)]\, \bar{C}_{ES}(i) + A_{ES} h_{ES} \left\{ [C_E(i,L) - C_S(i)] + \bar{C}_{ES}(i) \frac{z(i)F}{RT} [\psi_E(L) - \psi_S] \right\}, \tag{3-10}$$

where A_{ES} is the basement membrane area open to the channel. In all the simulations that follow we shall assume that there is no net transepithelial current flow, i.e., an open-circuited preparation. To achieve this we let serosal voltage, ψ_S, be a dependent variable and require

$$0 = \sum_i z(i)\,[F_{kE}(i,L) + F_{kI}(i,L)]. \tag{3-11}$$

Finally, the compliant features of the epithelium are incorporated into the relations

$$A_E(x) = (A_E(x))_0 [1 + \mu(P_E(L) - P_I(L) - ((P_E(L))_0 - (P_I(L))_0))], \tag{3-12}$$

$$L = (L)_0 [1 + \mu_L (P_I(0) - (P_I(0))_0)], \tag{3-13}$$

where both channel cross-section and epithelial height vary linearly as a function of an appropriate hydrostatic pressure. The values subscripted $(\,)_0$ indicate the reference at level flow. In the interest of enhanced numerical accuracy, we have specified uniform channel area for $0 < x < L$.

As in previous work (Weinstein & Stephenson, 1979), the model equations were cast as a spatially centered finite difference scheme and all variables determined simultaneously using Newton's method. This method has been carefully tested, particularly on large kidney models (Mejia, Stephenson & LeVeque, 1980). It has been found to be efficient and accurate, giving the same results as other tested boundary value problem solvers. It has also been compared on epithelial models with quasilinearization computational schemes (Huss & Stephenson, 1979). The parameter choices used for the *Necturus* and rabbit gallbladder simulations are indicated in the appendix in Tables A1-*A* and A2-*A*. Displayed in Tables A1-*B* and A2-*B* are the solutions of the model equations with each parameter set for the case of equal bathing media.

In addition to the reference parameters, several modified sets have been utilized in our experimental simulations with the aim of illustrating the effect of basement membrane solute permeability and mucosal membrane water permeability on epithelial function. For the *Necturus* experiments, all calculations have been carried out for each of the three channel basement membrane solute permeabilities, $(H_{ES}(i))$, multiplied by 5.0, 1.0, 0.2, and 0.04. Variation in mucosal water permeability has been performed in the rabbit simulations by multiplying the cell apical membrane, cell lateral membrane, and tight junction water permeabilities (L_{pMI}, L_{pIE}, L_{pME}) by 1.0, 0.1, 0.04, 0.02, and 0.01. The level-flow transepithelial fluxes and coupling coefficients for all nine parameter sets are indicated in Table 5. It is clear from the Table that with decreasing basement membrane solute permeability or increasing mucosal water permeability there is enhanced solute-solvent coupling. Furthermore, as was indicated for the compartmental channel model, the level flow reabsorbate tonicity, $(C_R)_0$, is not sufficient to decide the issue of isotonic transport.

By solving the model equations after imposing small increments of NaCl concentration in either mucosal or serosal boundary data ($\Delta C = 0.2$ mOsm/liter in *Necturus* experiments; 2.0 mOsm/liter in rabbit experiments) we may compute numerically the derivatives of the transepithelial fluxes with respect to these data. Then, following the analysis of Section 1, we may use these derivatives to estimate the deviations from isotonic transport. By imposing a small increment of an impermeant species within the mucosal bath one obtains an estimate of the whole epithelial hydraulic conductivity, namely $RTL_p = -\partial J_v / \partial C_i$. Finally, using $(J_v)_0$ and $\partial J_v / \partial C_M$, one may

Table 5. Level-flow properties predicted by the comprehensive epithelial model

	$(J_v)_0$[a] (nliter/sec cm^2)	$(J_s)_0$[b] (nOsm/sec cm^2)	$(C_R)_0$ (mOsm/liter)	γ
Necturus				
$H_B \times 5.0$	0.56	0.36	646	0.31
Reference	0.98	0.37	378	0.53
$H_B \times 0.2$	1.45	0.40	275	0.73
$H_B \times 0.04$	1.75	0.43	246	0.81
Rabbit				
Reference	17.47	4.09	234	0.85
$L_M \times 0.1$	13.61	4.10	301	0.66
$L_M \times 0.04$	10.36	4.08	394	0.51
$L_M \times 0.02$	7.66	4.06	530	0.38
$L_M \times 0.01$	5.19	4.04	778	0.26

[a] $J_v = F_{vE}(L) + F_{vI}(L)$.

[b] $J_s = \sum_{i=1}^{3} F_{kE}(i, L) + F_{kI}(i, L)$.

Table 6. Flux variation produced by small changes in the bathing media

	RTL_p[a] $\times 10^4$	$\frac{\partial J_v}{\partial C_M}$[a] $\times 10^4$	$\frac{\partial J_v}{\partial C_S}$[a] $\times 10^4$	$\frac{\partial J_s}{\partial C_M}$[b] $\times 10^6$	$\frac{\partial J_s}{\partial C_S}$[b] $\times 10^6$
Necturus					
$H_B \times 5.0$	9.98	−8.95	9.25	−6.74	8.90
Reference	7.52	−6.61	6.70	−4.66	6.42
$H_B \times 0.2$	5.07	−4.28	4.29	−2.12	3.92
$H_B \times 0.04$	4.05	−3.31	3.31	−0.96	3.06
Rabbit					
Reference	8.68	−6.95	7.17	22.18	−2.42
$L_M \times 0.1$	5.58	−4.47	4.63	21.97	−2.02
$L_M \times 0.04$	3.76	−2.97	3.09	22.90	−2.96
$L_M \times 0.02$	2.53	−1.97	2.07	23.67	−3.72
$L_M \times 0.01$	1.60	−1.23	1.31	24.31	−4.31

[a] (ml/sec cm^2)/(mOsm/cm^3).

[b] (mOsm/sec cm^2)/(mOsm/cm^3).

estimate the strength of transport, $\hat{C}$. For the parameter sets of interest, the numerical derivatives are displayed in Table 6, and the predicted concentrations C_M^*, C^*, C_S^*, and $\hat{C}$ in Table 7. It is worth noting in Table 6 that as predicted by the compartment model (Table 3) the L_p of rabbit gallbladder is more sharply dependent upon mucosal water permeability for the smaller values of mucosal water permeability. Put conversely, as mucosal water permeability increases, interspace solute polarization effects play a greater role in determining epithelial L_p. It may also be observed that for both models $\partial J_s/\partial C_M \doteq -\partial J_s/\partial C_S$, reflecting the asymmetry of the cell sodium transport law.

Examination of Table 7 reveals that all the *Necturus* parameter sets as well as the reference rabbit parameters are compatible with an isotonically transporting model. The *Necturus* experiments demonstrate that the osmotic deviations are remarkably insensitive to variations in basement membrane solute permeability - a fact suggested from the analytical study of the compartment model. The osmotic deviations are, however, quite dependent upon the mucosal water permeability.

It remains, therefore, to assess the accuracy of the estimates of the linear analysis by computing the osmotic deviations and strength of transport numerically. Thus, for example, C_M^* is determined by first solving the model equations for a range of mucosal bath salt concentrations to obtain a curve $C_R(C_M)$. The intersection of $C_R(C_M)$ with the line $C_R = C_M$ is just the point at which $C_M = C_M^*$ (calculated by linear interpolation from $C_R(C_M)$). Similar procedures yield

Table 7. Concentrations estimated from the linear analysis (mOsm/liter)

	C_M^*	C^*	C_S^*	$\hat{C}$
Necturus				
$H_B \times 5.0$	−1.44	−1.44	1.40	0.62
Reference	−1.38	−1.37	1.35	1.48
$H_B \times 0.2$	−1.31	−1.29	1.29	3.38
$H_B \times 0.04$	−1.27	−1.23	1.24	5.30
Rabbit				
Reference	−4.14	−3.69	3.64	25.14
$L_M \times 0.1$	−14.10	−12.38	12.74	30.47
$L_M \times 0.04$	−27.93	−24.41	26.69	34.94
$L_M \times 0.02$	−45.64	−40.10	47.87	38.88
$L_M \times 0.01$	−68.60	−61.32	84.21	42.13

C^* and C_S^*; $\hat{C}$ is the x-intercept of $J_v(C_M)$ as C_M is made increasingly hypertonic. Table 8 lists the results of these calculations, which are presented graphically in Figs. 5–7.

Figure 5 shows a set of experiments on the *Necturus* model. In the left panel, $C_R(C_M)$ is plotted as a solid curve as the mucosal bath osmolality varies from 194 to 200 mOsm/liter. (Serosal tonicity is fixed at 200 mOsm/liter); the four curves represent the four parameter sets. In the right panel, mucosal osmolality is fixed at 200 mOsm/liter and reabsorbate tonicity is plotted as a function of serosal concentration. The dashed line in the left panel is just $C_R = C_0 + C_M$; on the right $C_R = C_0 + C_S$. The approximately common point of intersection of the four curves with the line of identity is a striking display of the relative independence of C_M^* and C_S^* from basement membrane

Table 8. Numerical determination of transport equilibrium concentrations

	C_M^*	C^*	C_S^*	$\hat{C}$
Necturus				
$H_B \times 5.0$	−1.33	−1.31	1.31	–
Reference	−1.33	−1.31	1.31	–
$H_B \times 0.2$	−1.31	−1.28	1.28	–
$H_B \times 0.04$	−1.27	−1.23	1.23	–
Rabbit				
Reference	−3.94	−3.51	3.55	50.02
$L_M \times 0.1$	−13.23	−11.25	11.54	51.15
$L_M \times 0.04$	−27.16	−21.87	22.82	50.82
$L_M \times 0.02$	−48.20	−36.26	38.97	50.05
$L_M \times 0.01$	−81.37	−56.93	65.08	48.56

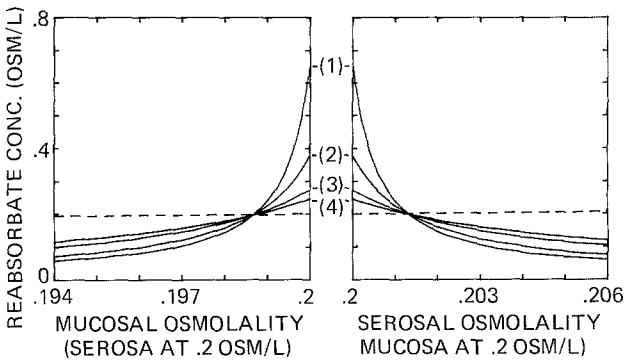

Fig. 5. Effect of bath osmolality on transport tonicity (*Necturus* parameters): In the left panel, reabsorbate concentration is plotted as a function of mucosal osmolality for four values of basement membrane solute permeability ((1) reference permeability × 5; (2) reference; (3) reference × 0.2, (4) reference × 0.04). The dashed line is the line $C_R = C_0 + C_M$. The intersection of a solid curve with the vertical line at C_0 is the value $C_R = (C_R)_0$; the intersection with the dashed line is $C_R = C_0 + C_M^*$. In the right panel, reabsorbate concentration is displayed as a function of serosal osmolality. The dashed line is $C_R = C_0 + C_S$, and the point of intersection with a solid curve is $C_R = C_0 + C_S^*$

solute permeability. With reference to Tables 7 and 8, one finds that for the reference parameter set, the predicted osmotic deviations are accurate to within 5 %.

Figure 6 displays the results of a similar set of experiments using the rabbit parameter sets. In the left panel, serosal osmolality is fixed at 200 mOsm/liter and mucosal osmolality is the independent variable. The intersection of $C_R(C_M)$ with the line of identity (short dashes) determines C_M^*. The right panel shows C_R as a function of C_S. These figures reveal both $(C_R)_0$ (the y-intercepts) and the osmotic deviations to be dependent on mucosal water permeability. Reference to the tabulated results shows the linear analysis accurate to 5 % for the reference parameters.

The transport of water against an adverse osmotic gradient by the rabbit epithelium is depicted in Fig. 7. With the serosa fixed at 200 mOsm/liter, mucosal

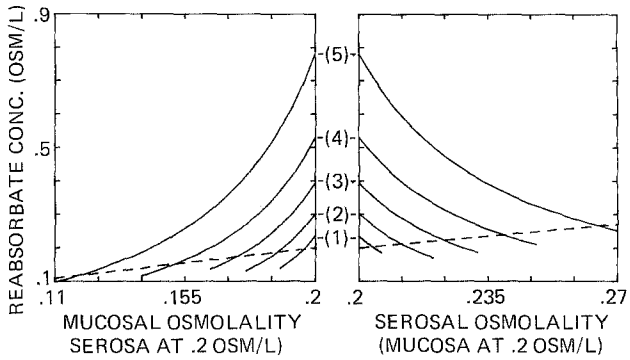

Fig. 6. Effect of bath osmolality on transport tonicity (rabbit parameters): In the left panel, reabsorbate concentration is plotted as a function of mucosal osmolality for five values of mucosal water permeability (1) reference; (2) reference × 0.1; (3) reference × 0.04; (4) reference × 0.02; (5) reference × 0.01). The dashed line is $C_R = C_0 + C_M$. Both $(C_R)_0$ and C_M^* are sensitive functions of L_M. In the right panel serosal osmolality is varied and C_S^* has been determined graphically

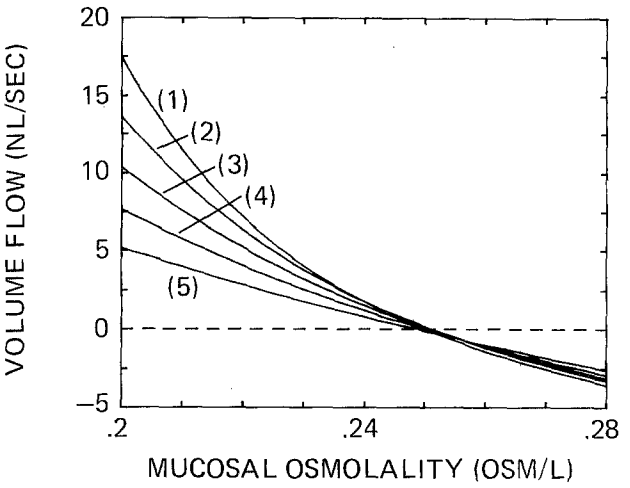

Fig. 7. Volume transport against an adverse osmotic gradient. The effect of increasing mucosal salt concentration on transepithelial volume flow is indicated for the rabbit model for five values of mucosal water permeability (*see* Fig. 6). As predicted by the compartment model, the strength of transport, $\hat{C}$, $(J_v(C_0 + \hat{C}) = 0)$ is quite insensitive to mucosal water permeability

bath osmolality is varied from 200 to 280 mOsm/liter and the computed J_v is plotted. As was suggested by even the elementary compartment model, the strength of transport (x-intercept) is remarkably independent of the mucosal water permeability – reflecting essentially solute transport rate and solute permeabilities of the lateral interspace. For these experiments, however, the strength of transport estimated from the linear analysis is substantially in error – reflecting important nonlinearities of a compliant epithelium.

Conclusion

The adequacy of a mathematical model used to represent a leaky epithelium should be measured against

at least three sets of experimental observations: (1) The model must predict near isotonicity of bathing media when either of the media is at osmotic equilibrium with the transport process. (2) The model's prediction of whole epithelial hydraulic conductivity should be comparable to that of the tissue. (3) The capacity of the tissue to transport water against an adverse osmotic gradient should be accurately simulated.

Quite general considerations of transport indicate that the assessment of the isotonicity of transport requires several sets of solutions of the model equations as the bathing media are varied about the point of equality. These calculations may yield either a direct numerical value for the osmotic deviations from isotonicity or else an estimate of the deviations using the computed transepithelial fluxes for equal bathing media and the derivatives of these fluxes with respect to bath osmolality. The single calculation with equal bathing media will, in general, not be sufficient to resolve the question of isotonicity. In particular, the reabsorbate tonicity for the epithelium betwen equal baths, $(C_R)_0$, may be quite a bit larger than the relevant osmotic deviations. Nevertheless, $(C_R)_0$ appears to be an important feature of epithelial performance and it is useful to define $\gamma = C_0/(C_R)_0$ the osmotic coupling coefficient of the epithelial model. It has been shown that the osmotic deviations may then be written as a product of two factors; $(1-\gamma)$, and another expression which appears to incorporate the solute and water permeabilities of the epithelium. Thus, the transport is "isotonic" for either a tightly coupled ($\gamma \approx 1$) or a sufficiently leaky system; the two effects are synergistic. Previous analyses in which tight coupling was a restriction imposed on models of isotonically transporting epithelia have resulted in difficulties with both compartmental and standing gradient type representations.

We have found a nonelectrolyte compartment model of the lateral intercellular space to be very useful in the simulation of epithelial transport in a variety of experimental settings. A linearization of the Kedem-Katchalsky equations about the condition of zero flow permits a straightforward calculation of the composite membrane properties from the component parameters. This linear version of the nonlinear compartment model is a numerically accurate approximation into the range of experimental interest and offers insight into the major determinants of steady-state phenomena in osmotic experiments.

It is found, for example, that intraepithelial solute polarization effects may profoundly influence the observed whole epithelial water permeabilities. This may serve to rationalize the discrepancy between the high cell membrane water permeabilities necessary to insure isotonic transport and the relatively low epithelial water permeabilities that have been measured in steady-state experiments.

Steady-state transport of water against an adverse osmotic gradient may also be adequately simulated with a compartment model of the interspace. It may be the case, however, that the parameter set relevant to this experiment is different from that used in the analysis of isotonic transport. The introduction of a compliance relation, by which channel area is determined by channel pressure, provides a rational basis by which to incorporate into the model the effects of the experimental procedure on tissue geometry.

Simulation of epithelial transport experiments with a polyelectrolyte distributed parameter model of interspace and cell largely confirms the qualitative predictions of the interspace compartment model. In particular, the deviations from reference for which either mucosal or serosal bath will be at transport equilibrium are shown to be independent of basement membrane solute permeability although crucially dependent on the water permeability of mucosal structures. Thus, in our understanding of the phenomenon of "isotonic transport" there appears to be little role for solute entrapment within the lateral intercellular space. In contrast, however, the capability of the epithelium to transport water against an osmotic gradient depends precisely on this ability to retain solute within the interspace in order to maintain the local hypertonicity required in the scheme of Curran and MacIntosh.

Appendix

Table A1-*A*. Parameter values for the rabbit epithelium[a]

I. Mobilities

	D_E (cm²/sec)	U_E $\left(\frac{\text{cm}^2}{\text{mvolt sec}}\right)$	D_I	U_I
Na	0.993×10^{-5}	0.384×10^{-6}	0.103×10^{-4}	0.399×10^{-6}
K	0.154×10^{-4}	0.597×10^{-6}	0.159×10^{-4}	0.614×10^{-6}
Cl	0.164×10^{-4}	-0.636×10^{-6}	0.151×10^{-4}	-0.584×10^{-6}

II. Dimensions

Apical cell cross-section 678 μ²
Apical cell membrane area (A_{MI}) 5 cm²/cm² epithelium
Apical channel area (A_{ME}) $= 1.85 \times 10^{-4}$ cm²/cm² epithelium
Cell perimeter (S) $= 2494$ cm/cm² epithelium
Cell height (cm)

[a] These parameters have been chosen quite arbitrarily so as to yield concentrations and fluxes compatible with data on rabbit gallbladder (*see* Table A1-B). Sufficient data from the literature is not available to justify this particular parameter set or exclude others.

Table A1-*A*. (cont.)

$L(t) = 0.002\,[1.0 + 0.8(P_I(0) - P_M)]$

Channel area (cm^2/cm^2 epithelium)

$A_E(x) = 0.056\,[1.0 + 0.13(P_E(L) - P_I(L))]$

Channel basement membrane area $A_{ES} = 0.2 \times A_E(L)$

Cell cross-section area $A_I(x) = 1.0 - A_E(x)$

III. Membrane characteristics

	Channel tight junction	Channel basement membrane	Cell apical	Cell basolateral
	L_{pME} (cm/sec mmHg)	L_{pES}	L_{pMI}	$L_{pIE} = 3.0 \times 10^{-7}$
	3.0×10^{-3}	1.2×10^{-4}	3.0×10^{-7}	$L_{pIS} = 2.0 \times 10^{-9}$
	σ_{ME}	σ_{ES}	σ_{MI}	$\sigma_{IE} = \sigma_{IS}$
Na	0.9	0.002	0.998	0.998
K	0.9	0.002	0.998	0.998
Cl	0.9	0.002	0.998	0.998

	H_{ME} (cm/sec)	H_{ES}	H_{MI}	$H_{IE} = H_{IS}$
Na	4.7×10^{-2}	1.0×10^{-2}	4.0×10^{-6}	1.0×10^{-10}
K	8.5×10^{-2}	1.0×10^{-2}	6.0×10^{-6}	1.0×10^{-5}
Cl	1.5×10^{-2}	1.0×10^{-2}	3.0×10^{-6}	4.0×10^{-6}

Apical NaCl co-transport is specified by the relations

$J_{MI}(\mathrm{Na}) = H_{MI}(\mathrm{Na})\,X_{MI}(\mathrm{Na}) + 0.8\,H_{MI}(\mathrm{Na})\,X_{MI}(\mathrm{Cl})$

$J_{MI}(\mathrm{Cl}) = 0.8 H_{MI}(\mathrm{Na})\,X_{MI}(\mathrm{Na}) + H_{MI}(\mathrm{Cl})\,X_{MI}(\mathrm{Cl})$

where $J_{MI}(i)$ and $X_{MI}(i)$ are the fluxes and driving forces and $H_{MI}(i)$ are permeability coefficients.

IV. The sodium pump at the lateral membrane

(mmol/sec cm channel cm^2 epithelium)

$NSP(\mathrm{Na}) = 6.0 \times 10^{-2}\,[C_I(\mathrm{Na}, L/2) - 0.008]$

$NSP(\mathrm{K}) = -0.8\,NSP(\mathrm{Na})$

Table A1-*B*. Steady-state solution for the open-circuited rabbit epithelium

	Intensive variables					
	Voltage (mV)	Pressure (mmHg)	Osmolality (Osm/l)	Concentration (mol/l)		
				Na	K	Cl
Mucosa	0.000	0.00	0.20000	0.09500	0.00500	0.10000
Channel	0.471	8.74	0.20101	0.09855	0.00196	0.10051
	0.472	8.74	0.20134	0.09865	0.00202	0.10067
	0.435	8.74	0.20114	0.09830	0.00227	0.10057
Cell	−57.17	0.07	0.20038	0.02660	0.07359	0.03801
	−57.17	0.07	0.20020	0.02643	0.07367	0.03792
	−57.17	0.07	0.20012	0.02638	0.07368	0.03788
Serosa	0.290	0.00	0.20000	0.09500	0.00500	0.10000
	Flows (per sq cm epithelium)					
	Current (mamp)		Volume flow (ml/sec)	Solute flow (mmol/sec)		
				Na	K	Cl
Channel	−0.298D-03		0.461D-05	−0.160D-08	0.484D-07	0.499D-07
	0.985D-02		0.986D-05	0.116D-05	−0.160D-06	0.901D-06
	0.178D-01		0.175D-04	0.233D-05	−0.394D-06	0.175D-05
Cell	0.298D-03		0.129D-04	0.233D-05	−0.333D-06	0.199D-05
	−0.985D-02		0.760D-05	0.117D-05	−0.124D-06	0.114D-05
	−0.178D-01		−0.825D-08	−0.181D-10	0.109D-06	0.294D-06

Reabsorbate tonicity = 0.234.

Values of the variables for channel and cell are given for $x = 0.0$ (mucosal boundary), $x = L/2$, and $x = L$(serosal boundary).

Table A2-*A*. Parameter values for the *Necturus* epithelium[a]

I. Mobilities

	D_E (cm^2/sec)	U_E $\left(\frac{cm^2}{mvolt\,sec}\right)$	D_I	U_I
Na	0.993×10^{-5}	0.384×10^{-6}	0.103×10^{-4}	0.399×10^{-6}
K	0.154×10^{-4}	0.597×10^{-6}	0.159×10^{-4}	0.614×10^{-6}
Cl	0.164×10^{-4}	-0.636×10^{-6}	0.151×10^{-4}	-0.584×10^{-6}

II. Dimensions

Apical cell cross-section 678 μ^2
Apical cell membrane area (A_{MI}) 5 cm^2/cm^2 epithelium
Apical channel area (A_{ME}) $=1.85\times10^{-4}$ cm^2/cm^2 epithelium
Cell perimeter (S) $=2494$ cm/cm^2 epithelium
Cell height (cm)

$L(t)=0.002\,[1.0+0.8(P_I(0)-P_M)]$

Channel area (cm^2/cm^2 epithelium)

$A_E(x)=0.056\,[1.0+0.13(P_E(L)-P_I(L))]$

Channel basement membrane area $A_{ES}=0.2\times A_E(L)$

Cell cross-section area $A_I(x)=1.0-A_E(x)$

[a] These parameters have been used in a previous model of *Necturus* gallbladder and have been justified in that paper (Weinstein & Stephenson, 1979).

III. Membrane characteristics

	Channel tight junction	Channel basement membrane	Cell apical	Cell basolateral
	L_{pME} (cm/sec mmHg)	L_{pES}	L_{pMI}	$L_{pIE}=L_{pIS}$
	3.0×10^{-4}	2.0×10^{-5}	2.0×10^{-8}	2.0×10^{-8}
	σ_{ME}	σ_{ES}	σ_{MI}	$\sigma_{IE}=\sigma_{IS}$
Na	0.8	0.002	0.998	0.998
K	0.7	0.002	0.998	0.998
Cl	0.8	0.002	0.998	0.998
	H_{ME} (cm/sec)	H_{ES}	H_{MI}	$H_{IE}=H_{IS}$
Na	4.7×10^{-2}	1.0×10^{-2}	4.0×10^{-7}	1.0×10^{-10}
K	8.5×10^{-2}	1.0×10^{-2}	6.0×10^{-7}	1.0×10^{-6}
Cl	1.5×10^{-2}	1.0×10^{-2}	3.0×10^{-7}	3.0×10^{-7}

Apical NaCl co-transport is specified by the relations

$J_{MI}(\mathrm{Na})=H_{MI}(\mathrm{Na})\,X_{MI}(\mathrm{Na})+0.8\,H_{MI}(\mathrm{Na})\,X_{MI}(\mathrm{Cl})$

$J_{MI}(\mathrm{Cl})\ =0.8\,H_{MI}(\mathrm{Na})\,X_{MI}(\mathrm{Na})+H_{MI}(\mathrm{Cl})\,X_{MI}(\mathrm{Cl})$

where $J_{MI}(i)$ and $X_{MI}(i)$ are the fluxes and driving forces and $H_{MI}(i)$ are permeability coefficients.

IV. The sodium pump at the lateral membrane

(mmol/sec cm channel cm^2 epithelium)

$NSP(\mathrm{Na})=7.5\times10^{-3}\,[C_I(\mathrm{Na}, L/2)-0.008]$

$NSP(\mathrm{K})\ =-0.8\,NSP(\mathrm{Na})$

Table A2-*B*. Steady-state solution for the open-circuited *Necturus* epithelium

	Intensive variables					
	Voltage (mV)	Pressure (mmHg)	Osmolality (Osm/l)	Concentration (mol/l)		
				Na	K	Cl
Mucosa	0.000	0.00	0.20000	0.09750	0.00250	0.10000
Channel	0.663	3.33	0.20074	0.09838	0.00199	0.10037
	0.666	3.33	0.20078	0.09839	0.00200	0.10039
	0.661	3.33	0.20069	0.09830	0.00204	0.10035
Cell	−62.07	0.05	0.20017	0.02448	0.07560	0.03746
	−62.07	0.05	0.20015	0.02446	0.07561	0.03745
	−62.07	0.05	0.20014	0.02445	0.07561	0.03745
Serosa	0.656	0.00	0.20000	0.09750	0.00250	0.10000
	Flows (per sq cm epithelium)					
	Current (mamp)	Volume flow (ml/sec)		Solute flow (mmol/sec)		
				Na	K	Cl
Channel	−0.274D-02	0.479D-06		−0.201D-07	0.749D-08	0.157D-07
	−0.105D-02	0.777D-06		0.108D-06	−0.317D-07	0.877D-07
	0.585D-03	0.107D-05		0.237D-06	−0.714D-07	0.160D-06
Cell	0.274D-02	0.500D-06		0.257D-06	−0.595D-07	0.169D-06
	0.105D-02	0.203D-06		0.129D-06	−0.203D-07	0.974D-07
	−0.585D-03	−0.892D-07		−0.279D-10	0.193D-07	0.254D-07

Reabsorbate tonicity = 0.378.
Values of the variables for channel and cell are given for $x=0.0$ (mucosal boundary), $x=L/2$, and $x=L$(serosal boundary).

References

Andreoli, T.E., Schafer, J.A. 1978. Volume absorption in the pars recta. III. Luminal hypotonicity as a driving force for isotonic volume absorption. *Am. J. Physiol.* **234**:F349

Andreoli, T.E., Schafer, J.A., Troutman, S.L. 1978. Perfusion rate-dependence of transepithelial osmosis in isolated proximal convoluted tubules: Estimation of the hydraulic conductance. *Kidney Int.* **14**:263

Curran, P.F., MacIntosh, J.R. 1962. A model system for biological water transport. *Nature (London)* **193**:347

Diamond, J.M. 1962. The reabsorptive function of the gall-bladder. *J. Physiol. (London)* **161**:442

Diamond, J.M. 1964*a*. Transport of salt and water in rabbit and guinea pig gall bladder. *J. Gen. Physiol.* **48**:1

Diamond, J.M. 1964*b*. The mechanism of isotonic water transport. *J. Gen. Physiol.* **48**:15

Diamond, J.M. 1966. Non-linear osmosis. *J. Physiol. (London)* **183**:58

Diamond, J.M. 1978. Solute-linked water transport in epithelia. *In:* Membrane Transport Processes. J.F. Hoffman, editor. pp. 257–276. Raven Press, New York

Diamond, J.M., Bossert, W.H. 1967. Standing-gradient osmotic flow. A mechanism for coupling of water and solute transport in epithelia. *J. Gen. Physiol.* **50**:2061

Henin, S., Cremaschi, D., Schettino, T., Meyer, G., Donin, C.L.L., Cotelli, F. 1977. Electrical parameters in gallbladders of different species. Their contribution to the origin of the transmural potential difference. *J. Membrane Biol.* **34**:73

Hill, A.E. 1975*a*. Solute-solvent coupling in epithelia: A critical examination of the standing-gradient osmotic flow theory. *Proc. R. Soc. London B.* **190**:99

Hill, A.E. 1975*b*. Solute-solvent coupling in epithelia: Contribution of the junctional pathway to fluid production. *Proc. R. Soc. London B.* **191**:537

Hill, A.E. 1977. General mechanisms of salt-water coupling in epithelia. *In:* Transport of Ions and Water in Animals. B. Gupta, R. Moreton, J. Oschman, and B. Wall, editors. pp. 183–214. Academic Press, Inc., New York

Hill, A.E., Hill, B.S. 1978*a*. Sucrose fluxes and junctional water flow across *Necturus* gall bladder epithelium. *Proc. R. Soc. London B.* **200**:163

Hill, B.S., Hill, A.E. 1978*b*. Fluid transfer by *Necturus* gall bladder epithelium as a function of osmolarity. *Proc. R. Soc. London B.* **200**:151

Huss, R.E., Marsh, D.J. 1975. A model of NaCl and water flow through paracellular pathways of renal proximal tubules. *J. Membrane Biol.* **23**:305

Huss, R.E., Stephenson, J.L. 1979. A mathematical model of proximal tubule absorption. *J. Membrane Biol.* **47**:377

Lin, C.C., Segel, L.A. 1974. Illustration of techniques on a physiological flow problem. *In:* Mathematics Applied to Deterministic Problems in the Natural Sciences. pp. 244–276. Macmillan, New York

Lutz, M.D., Cardinal, J., Burg, M.B. 1973. Electrical resistance of renal proximal tubule perfused *in vitro*. *Am. J. Physiol.* **225**:729

Mejia, R., Stephenson, J.L., LeVeque, R.J. 1980. A test problem for kidney models. *Math. Biosci.* **50**:129

Mikulecky, D.C. 1977. A simple network thermodynamic method for series-parallel coupled flows: II. The non-linear theory, with applications to coupled solute and volume flow in a series membrane. *J. Theoret. Biol.* **69**:511

Mikulecky, D.C., Thomas, S.R. 1978. A simple network thermodynamic method for series-parallel coupled flows: III. Application to coupled solute and volume flows through epithelial membranes. *J. Theoret. Biol.* **73**:697

Mikulecky, D.C., Wiegand, W.A., Shiner, J.S. 1977. A simple network thermodynamic method for modeling series-parallel coupled flows: I. The linear case. *J. Theoret. Biol.* **69**:471

Patlak, C.S., Goldstein, D.A., Hoffman, J.F. 1963. The flow of solute and solvent across a two-membrane system. *J. Theoret. Biol.* **5**:426

Reuss, L., Finn, A.L. 1977. Effects of luminal hyperosmolality on electrical pathways of *Necturus* gallbladder. *Am. J. Physiol.* **232**:C99

Sackin, H., Boulpaep, E.L. 1975. Models for coupling of salt and water transport. Proximal tubular reabsorption in *Necturus* kidney. *J. Gen. Physiol.* **66**:671

Segel, L.A. 1970. Standing-gradient flows driven by active solute transport. *J. Theoret. Biol.* **29**:233

Sha'afi, R.I., Rich, G.T., Sidel, V.W., Bossert, W., Solomon, A.K. 1967. The effect of the unstirred layer on human red cell water permeability. *J. Gen. Physiol.* **50**:1377

Smulders, A.P., Tormey, J.M., Wright, E.M. 1972. The effect of osmotically induced water flows on the permeability and ultrastructure of the rabbit gallbladder. *J. Membrane Biol.* **7**:164

Spring, K.R., Hope, A. 1978. Size and shape of the lateral intercellular spaces in a living epithelium. *Science* **200**:54

Spring, K.R., Hope, A. 1979*a*. Dimensions of cells and lateral intercellular spaces in living *Necturus* gallbladder. *Fed. Proc.* **38**:128

Spring, K.R., Hope, A. 1979*b*. Fluid transport and the dimensions of cells and interspaces of living *Necturus* gallbladder. *J. Gen. Physiol.* **73**:287

Thomas, S.R., Mikulecky, D.C. 1978. A network thermodynamic model of salt and water flow across the kidney proximal tubule. *Am. J. Physiol.* **235**:F638

Tormey, J.M., Diamond, J.M. 1967. The ultrastructural route of fluid transport in rabbit gall bladder. *J. Gen. Physiol.* **50**:2031

Weinstein, A.M., Stephenson, J.L. 1978. Transport across a simple epithelium. *FASEB, 62nd Annual Meeting.* Atlantic City, N.J., April 9–14. Abstract, p. 569

Weinstein, A.M., Stephenson, J.L. 1979. Electrolyte transport across a simple epithelium. Steady-state and transient analysis. *Biophys. J.* **27**:165

Welling, L.W., Grantham, J.J. 1972. Physical properties of isolated perfused renal tubules and tubular basement membranes. *J. Clin. Invest.* **51**:1063

Welling, L.W., Welling, D.J. 1975. Surface areas of brush border and lateral cell walls in the rabbit proximal nephron. *Kidney Int.* **8**:343

Whitlock, R.T., Wheeler, H.O. 1964. Coupled transport of solute and water across rabbit gallbladder epithelium. *J. Clin. Invest.* **48**:2249

Wright, E.M., Diamond, J.M. 1968. Effects of pH and polyvalent cations on the selective permeability of gall-bladder epithelium to monovalent ions. *Biochim. Biophys. Acta* **163**:57

Wright, E.M., Smulders, A.P., Tormey, J.M. 1972. The role of the lateral intercellular spaces and solute polarization effects in the passive flow of water across the rabbit gallbladder. *J. Membrane Biol.* **7**:198

Received 19 February 1980; revised 18 November 1980